Communication

Anion-Receptor Mediated Oxidation of Carbon Monoxide to Carbonate by Peroxide Dianion

Journal of the American Chemical Society is published by the American Chemical Society. 1155 Sixteenth Street N.W., Washington, DC 20036

Matthew Nava, Nazario Lopez, Peter
Müller, Gang Wu, Daniel G. Nocera,
and Christopher C. Cummins

J. Am. Chem. Soc., **Just Accepted Manuscript** • DOI: 10.1021/jacs.5b08495 • Publication Date (Web): 14 Oct 2015

Journal of the American Chemical Society is published by the American Chemical Society. 1155 Sixteenth Street N.W., Washington, DC 20036
Published by American Chemical Society.

Journal of the American Chemical Society is published by the American Chemical Society. 1155 Sixteenth Street N.W., Washington, DC 20036
Published by American Chemical Society. Copyright © American Chemical Society. However,

Journal of the American
Chemical Society is
published by the American
Chemical Society. 1155
Sixteenth Street N.W.,
Washington, DC 20036

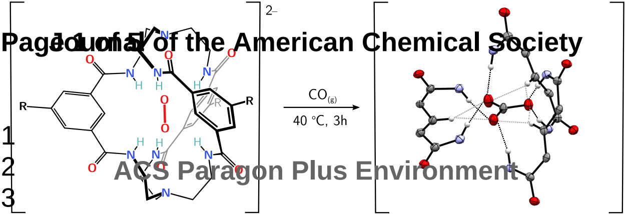

Encapsulated Peroxide

Encapsulated Carbonate Cutaway

Anion-Receptor Mediated Oxidation of Carbon Monoxide to Carbonate by Peroxide Dianion

Matthew Nava,[†] Nazario Lopez,[†,‡] Peter Müller,[†] Gang Wu,[¶] Daniel G. Nocera,[*,§] and Christopher C. Cummins[*,†]

†Department of Chemistry, Massachusetts Institute of Technology, Cambridge MA, United States 02139-4307, ‡Current Address: Centro de Investigaciones Químicas, IICBA, Universidad Autonoma del Estado de Morelos, Avenida Universidad 1001, Colonia Chamilpa, C.P. 62209, Cuernavaca, Morelos Mexico, ¶Department of Chemistry, Queen's University, 90 Bader Lane, Kingston ON, Canada K7L3N6, and §Department of Chemistry and Chemical Biology, Harvard University, 12 Oxford Street, Cambridge MA, United States

Received October 10, 2015; E-mail: dnocera@fas.harvard.edu; ccummins@mit.edu

Abstract: The reactivity of peroxide dianion $O_2{}^{2-}$ has been scarcely explored in organic media due to the lack of soluble sources of this reduced oxygen species. We now report the finding that the encapsulated peroxide cryptate, $[O_2{\subset}m\text{BDCA-5t-H}_6]^{2-}$(**1**), reacts with carbon monoxide in organic solvents at 40 °C to cleanly form an encapsulated carbonate. Characterization of the resulting hexacarboxamide carbonate cryptate by single crystal X-ray diffraction reveals that carbonate dianion forms nine complementary hydrogen bonds with the hexacarboxamide cryptand, $[CO_3{\subset}m\text{BDCA-5t-H}_6]^{2-}$(**2**), a conclusion that is supported by spectroscopic data. Labeling studies and ^{17}O solid-state NMR data confirm that two thirds of the oxygen atoms in the encapsulated carbonate derive from peroxide dianion while the carbon is derived from CO. Further evidence for the formation of a carbonate cryptate was obtained by three methods of independent synthesis: treatment of (*i*) free cryptand with K_2CO_3; (*ii*) monodeprotonated cryptand with PPN[HCO_3]; and (*iii*) free cryptand with TBA[OH] and atmospheric CO_2. This work demonstrates CO oxidation mediated by a hydrogen-bonding anion receptor, constituting an alternative to transition-metal catalysis.

The reduction of carbon dioxide to carbon monoxide, formate, alcohols or alkanes has garnered considerable attention, especially when coupled with renewable energy sources as a means to reduce humanity's dependence on fossil fuels.[1] The reverse reaction, oxidation of carbon monoxide to carbon dioxide is also an important transformation due to toxicity of CO and the need to mitigate CO from industrial waste streams and vehicle exhaust.[2] This transformation can be effected by soluble metal complexes and heterogeneous systems, with gold nanoparticles being the most active catalyst in the oxidation to CO_2.[3] Numerous other heterogeneous systems exist that are capable of oxidizing CO to CO_2 at room temperature or more commonly at elevated temperatures with an important example being the transition metal oxide Hopcalite.[4] Well-defined molecular complexes that can oxidize CO to carbonate can be divided into two distinct categories: (*i*) low oxidation-state metal carbonyl complexes that reduce free O_2 to peroxide, which subsequently reacts with a coordinated carbonyl ligand,[5] and (*ii*) peroxo metal complexes that couple with free CO.[6]

A fundamental question that to date has not been addressed is concerned with the reactivity of peroxide dianion *on its own* towards CO; the insolubility of alkali metal peroxides in polar aprotic organic media hampers direct testing of this reaction. Recent experimental and theoretical work has demonstrated that peroxide and superoxide on the surface of metal oxide materials are able to oxidize CO to CO_2 or surface-bound $CO_3{}^{2-}$.[7–9] Ceria, which is used in automobile catalytic converters, is a prominent example of this type of reactivity as it has been shown experimentally and computationally to oxidize CO to carbonate upon reaction with peroxide.[9,10] When studying metal oxide systems it is often difficult to uncouple the reactivity of peroxide dianion with CO from the reactivity of the supporting metal. In this work, we report the oxidation of CO by a peroxide dianion[11,12] isolated in a hydrogen bonding anion receptor $[O_2{\subset}m\text{BDCA-5t-H}_6]^{2-}$ (**1**),[13] resulting in the formation of an encapsulated carbonate cryptate $[CO_3{\subset}m\text{BDCA-5t-H}_6]^{2-}$ (**2**). As in the case of peroxide cryptate **1** and other systems in which an anion is sequestered in the inner space of hexacarboxamide cryptand constructs,[14] the carbonate dianion in **2** is encased by the sheath of multiple hydrogen-bond donors that constitute the anion receptor's interior lining.

Exposure of a yellow solution of $[(\text{TBA})_2]$ [**1**][15] to CO (1 atm, 3 h, 40 °C) in a THF-DMF mixture (10:1 v:v) results in the formation of carbonate adduct $[(\text{TBA})_2]$ [**2**] in quantitative yield. The ^{1}H NMR spectrum of **2** is characterized by distinct downfield chemical shifts of the internally directed N-H carboxamide protons of the cryptand as well as the central C-H aryl protons, analogous to the ^{1}H NMR spectroscopic signatures for **1** and indicative of strong hydrogen bonding interactions (Figure 1). Proton NMR signals for the carbonate anion cryptate were observed at 12.2 ppm (N-H protons); these signals are downfield from those observed for the free cryptand (8.65 ppm). In addition, the internally directed aryl C-H protons are found at 10.8 ppm in contrast with the ^{1}H NMR signals of the peroxide anion cryptate (10.10 ppm) and the free cryptand (8.60 ppm). Preparation of the carbonate anion cryptate from ^{13}CO and **1** resulted in an intense ^{13}C NMR signal at 172.4 ppm, within the expected region for carbonate dianion ensconced in an anion receptor,[16] showing that CO is the source of carbon in carbonate anion cryptate.

Single crystals suitable for an X-ray diffraction study were obtained by vapor diffusion of diethyl ether into a THF solu-

---

[†] Massachusetts Institute of Technology

[‡] Universidad Autonoma del Estado de Morelos

[¶] Queen's University

[§] Harvard University

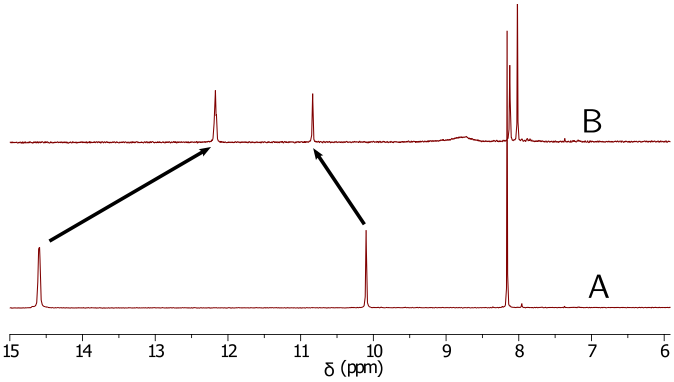

Figure 1. ^{1}H NMR spectrum of $[(\mathrm{TBA})_2][\mathrm{O_2}\subset m\mathrm{BDCA\text{-}5t\text{-}H_6}]$ (A) and $[(\mathrm{TBA})_2][\mathrm{CO_3}\subset m\mathrm{BDCA\text{-}5t\text{-}H_6}]$ (B) in DMSO-d$_6$ after exposure to CO gas (40 °C, 3 h).

tion of $[(\mathrm{TBA})_2]$ [**2**]; the sample originated directly from CO treatment of a solution of $[(\mathrm{TBA})_2]$ [**1**]. A view along the pseudo-three fold axis of the carbonate anion cryptate indicates that the cryptand retains the propeller like (D_3) conformation observed in the peroxide dianion cryptate but the plane of the $[\mathrm{CO_3}]^{2-}$ unit is perpendicular to the cryptand pseudo-C_3 axis (the peroxide dianion in **1** lies along the cryptand pseudo-C_3 axis). The cryptand is slightly more compressed along its pseudo-C_3 axis in the carbonate anion cryptate relative to the peroxide cryptate, highlighting the conformational flexibility of the hexacarboxamide cryptand, which adjusts its conformation depending on the shape of the anion bound in its cavity. A total of six N-H carboxamide hydrogen bonds are made to the three oxygen atoms of the carbonate with N···O distances ranging from 2.613 - 2.977 Å (average distance 2.75 Å), characteristic of intermediate strength hydrogen bonds.[17] Also evident from the crystal structure is the presence of bifurcated cryptand phenylene C-H···O interactions with the carbonate oxygens, as noted previously in other anionic adducts of hexacarboxamide cryptand systems.[11,14,18]

The solid-state ^{17}O NMR spectra for $[\mathrm{K_2(DMF)_2}][\mathrm{CO^{17}O_2}\subset m\mathrm{BDCA\text{-}5t\text{-}H_6}]$ (**3**) prepared from mBDCA-5t-H$_6$, $^{17}\mathrm{O}_2$ and a reducing agent followed by treatment with CO (Scheme 1) are shown in Figure 4.[19] At 298 K, the ^{17}O NMR spectrum exhibits a relatively narrow but featureless peak centered at 150 ppm. This spectral feature suggests the presence of significant molecular motion for the encapsulated carbonate anion even in the solid state. To further probe this molecular motion, ^{17}O solid-state NMR spectra were collected at different temperatures. At 223 K, as seen in Figure 4, the ^{17}O NMR spectrum of **3** now shows a regular line shape commonly observed in solid-state ^{17}O NMR spectra, arising from a combination of second-order quadrupolar interactions and chemical shift anisotropy.[20] Analysis of this low-temperature spectrum yielded the following parameters for **3**: C_Q = 7.5 MHz, η_Q = 0.7, δ_{iso} = 170, δ_{11} = 266, δ_{22} = 194, δ_{33} = 50 ppm. These spectral parameters are similar to those reported for $\mathrm{CaCO_3}$[21] and $\mathrm{Li_2CO_3}$.[22] To further establish the identity of the carbonate anion in the adduct, we used the Amsterdam Density Functional (ADF) program to perform quantum chemical computations of the ^{17}O NMR parameters for a $[\mathrm{CO_3}\subset m\mathrm{BDCA\text{-}5t\text{-}H_6}]^{2-}$ model generated from the crystal structure of the anion cryptate.[19] The ADF computational results are: C_Q = 7.03 MHz, η_Q = 0.95, δ_{iso} = 223, δ_{11} = 335, δ_{22} = 222, δ_{33} = 112 ppm. These calculated ^{17}O NMR parameters are in reasonably good agreement with the experimental results discussed above.

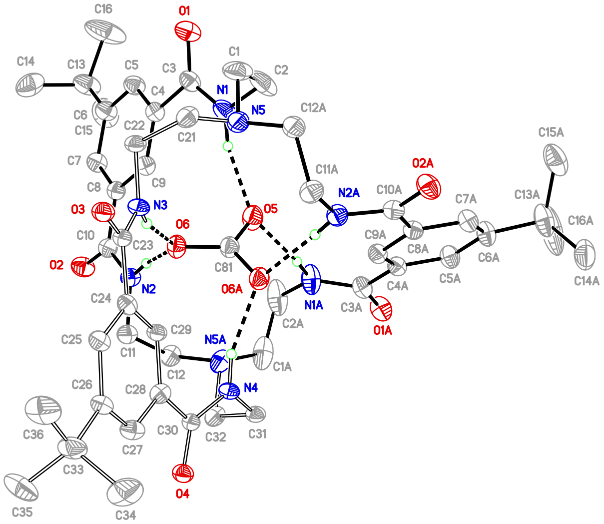

Figure 2. Solid-state structure of $[(\mathrm{TBA})_2][\mathrm{CO_3}\subset m\mathrm{BDCA\text{-}5t\text{-}H_6}]$ with thermal ellipsoids plotted at the 50% probability level. Counter cations, solvent and all hydrogen atoms are omitted for clarity except for the N-H carboxamide protons engaged in hydrogen bonding with the carbonate anion. Selected interatomic distances (Å) and angles (°): C81-O(carbonate) 1.291(avg), N5-N5A 7.687(2), N1-O5 2.739, N2-O6 2.754(2), N3-O6 2.72(2), N4-O6A 2.79(1), O5-C81-O6 120.2°, O6-C81-O6A 119.7°, C9-O6 3.151(1), C9-O5 3.257, C29-O6 3.14(1) C29-O6A 3.19(1)

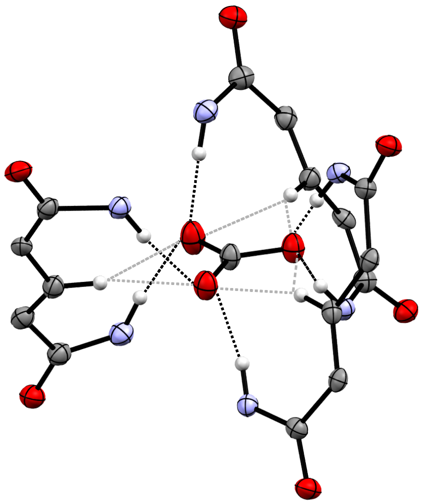

Figure 3. Cutway of **2** illustrating the inner hydrogen-bonding sheath of the hexacarboxamide cryptand and the interactions with carbonate dianion. NH···O hydrogen bonds are indicated by black lines while bifurcated CH···O hydrogen bonds are indicated by light gray lines.

$$\begin{aligned} & m\mathrm{BDCA\text{-}5t\text{-}H_6} + {}^{17}\mathrm{O_2} + 2\mathrm{K(TEMPO)} \xrightarrow[\mathrm{DMF}]{23\ ^\circ\mathrm{C,\ 3\ h}} \\ & [\mathrm{K_2(DMF)_3}][{}^{17}\mathrm{O_2}\subset m\mathrm{BDCA\text{-}5t\text{-}H_6}] + \mathrm{CO} \xrightarrow[\mathrm{DMF}]{23\ ^\circ\mathrm{C,\ 24\ h}} \\ & \underset{\mathbf{3}}{[\mathrm{K_2(DMF)_2}][\mathrm{CO^{17}O_2}\subset m\mathrm{BDCA\text{-}5t\text{-}H_6}]} \end{aligned} \tag{1}$$

Furthermore, as shown in Figure 4, we were able to analyze the experimental variable-temperature ^{17}O NMR spectra by assuming that the carbonate anion undergoes discrete jumps about its C_3 axis, a dynamic process resembling a

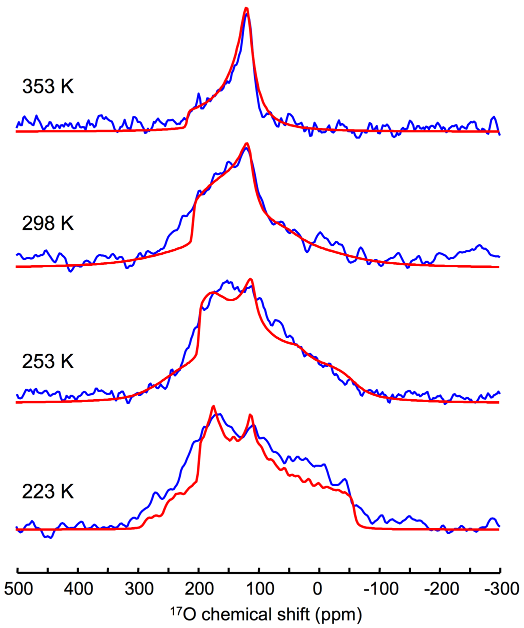

Figure 4. Experimental (blue) and simulated (red) solid-state ^{17}O NMR spectra of $[K_2(DMF)_2][CO^{17}O_2{\subset}m\text{BDCA-5t-H}_6]$ at different temperatures. All spectra were recorded at 14.1 T.

molecular gyroscope.[23] Our analysis of the solid state ^{17}O NMR data shown in Figure 4 yielded the activation energy for such jumps, E_a=22±2 kJ mol^{-1}(see figure S21). It is interesting to note that each of the three carbonate oxygen atoms form two O ⋯ H-N hydrogen bonds (r_{o-n}=2.80 Å) inside the cryptand cage. Therefore, in order for the encapsulated carbonate to rotate, a total of six O ⋯ H-N hydrogen bonds must break. We also note that the observed activation energy for the carbonate jumps is smaller than those found for the three-fold jumps for the -$SO_3{}^{-1}$ group in crystalline sulfonic acids,[24] reflecting the fact that the hydrogen bonding strength is greater in the latter cases which contain more ionic O ⋯ H-N hydrogen bonds. The current case represents a very rare instance wherein carbonate anion dynamics are probed directly by solid-state ^{17}O NMR spectroscopy. This also illustrates the unique information that ^{17}O NMR spectroscopy can offer, as ^{13}C NMR would be insensitive to the aforementioned dynamics.

The carbonate anion cryptate can also be prepared by alternative routes in support of the carbonate assignment. Treatment of monodeprotonated cryptand with PPN[HCO_3] (i)[25] leads to proton transfer from bicarbonate to the cryptand and subsequent encapsulation of carbonate. In addition, free cryptand can be treated with excess potassium carbonate (ii) as a slurry in an organic solvent resulting in the isolation of the carbonate anion cryptate along with 20% free cryptand. Excess potassium carbonate is required due to the presumed equilibrium of solid potassium carbonate with encapsulated carbonate cryptate. Alternatively, exposure of a solution of free cryptand and TBA[OH] in methanol to an ambient atmosphere (iii) also led to the clean production of the carbonate anion cryptate. Carbonate in the latter case is presumably derived from nucleophilic attack of hydroxide ion on atmospheric CO_2, as is precedented in anion recognition chemistry.[16,26–28]

$$\underset{\textbf{i}}{[\mathrm{K(DMF)}_x][m\mathrm{BDCA\text{-}5t\text{-}H_5}]} + [\mathrm{PPN}][\mathrm{HCO_3}] \xrightarrow[\mathrm{DMF}]{23\ ^\circ\mathrm{C},\ 14\ \mathrm{h}} [(\mathrm{PPN})\mathrm{K}][\mathbf{2}]$$

$$\underset{\textbf{ii}}{m\mathrm{BDCA\text{-}5t\text{-}H_6}} + \mathrm{K_2CO_3} \xrightarrow[\mathrm{DMF}]{23\ ^\circ\mathrm{C},\ 48\ \mathrm{h}} [\mathrm{K_2(DMF)}_x][\mathbf{2}]$$

$$\underset{\textbf{iii}}{m\mathrm{BDCA\text{-}5t\text{-}H_6}} + \mathrm{TBAOH} \xrightarrow[\mathrm{DMF}]{23\ ^\circ\mathrm{C},\ 1\ \mathrm{h,\ air}} [(\mathrm{TBA})_2][\mathbf{2}] \qquad (2)$$

If potassium rather than TBA is used to prepare the carbonate anion cryptate, the ^{1}H NMR spectrum taken after precipitation of the product with Et_2O indicates a mixture of carbonate anion cryptate and free cryptand in typical ratios of 80:20. The formation of free cryptand is likely the result of carbonate extraction from the cryptand by potassium ions, explaining the observation (mentioned above) that the carbonate anion cryptate cannot be prepared in quantitative yield directly from potassium carbonate. Addition of several equivalents of potassium triflate to a solution of the tetrabutylammonium salt of carbonate anion cryptate in DMF-d_7 was also found to induce the formation of free cryptand and by inference potassium carbonate illustrating the cation's role with respect to the stability of the carbonate peroxide adduct.[19] Tetrabutylammonium salts of the carbonate anion cryptate are not indefinitely stable in solution, and over time deprotonated cryptand is observed likely stemming from the formation of bicarbonate or carbonic acid which decomposes to release water and CO_2 and may account for the observed water molecule in the crystal structure of the carbonate anion cryptate.

Isotopic labeling studies were conducted to confirm the origin of the atoms in the carbonate anion cryptate. In particular, to verify that the proposed reaction of peroxide and CO occurs and that ensuing carbonate is not a byproduct of a side reaction or impurity, we sought to confirm that the carbonate carbon is derived from CO and that two-thirds of the oxygen atoms are derived from the oxygen atoms in the peroxide dianion cryptate. The latter was therefore prepared utilizing $^{18}O_2$ and the labeled material so obtained was then exposed to $^{13}C^{16}O$. Evidence for the formation of a labeled carbonate anion cryptate $[^{13}CO^{18}O_2{\subset}m\text{BDCA-5t-H}_6]^{2-}$ was obtained from the decomposition of the carbonate adduct by treatment with two equivalents of HBF_4, in order to form carbonic acid *in situ* with ensuing conversion to water and evolved gas identified as CO_2. Release of $^{13}C^{18}O_2$ and $^{13}C^{18}O^{16}O$ was confirmed by headspace sampling with an EI quadrupole mass spectrometer demonstrating that $^{18}O_2{}^{2-}$ reacts with ^{13}CO. $^{13}C^{16}O_2$ was also observed and in a control experiment, it was found that adding a small amount of water ($H_2{}^{18}O$) to ^{16}O labeled carbonate followed by acid decomposition resulted in a substantial decrease in the $C^{16}O_2$ signal and appearance of $C^{18}O_2$ and $C^{16}O^{18}O$, providing a possible explanation for the loss of some of the ^{18}O when starting from ^{18}O labeled peroxide.

While the reaction of CO with peroxide dianion in solution has not been reported previously, CO has been demonstrated to react with hydrogen peroxide[29–31] upon photolysis at room temperature to produce CO_2. Detailed kinetic studies demonstrate that the reaction proceeds first through O-O bond homolysis of hydrogen peroxide generating hydroxy radicals (·OH) which then react with CO under a radical chain mechanism. Further evidence that the hydroxyl radical is able to rapidly oxidize CO was obtained through electrochemical studies using boron doped diamond electrodes.[32] In both of the aforementioned examples, peroxide dianion is not implicated as the oxidant and thus far represent the few examples of metal free oxidations of CO to yield CO_2.

The results presented herein demonstrate that peroxide dianion is able to react with CO without the assistance of a transition metal. Currently, it is unclear what role cryptand *m*BDCA-5t-H_6 plays in the transformation besides functioning as a solubilizing agent for the peroxide dianion and as a host for the carbonate dianion reaction product. *In situ* generation of hydrogen peroxide via proton transfer from the cryptand is ruled out on the basis that H_2O_2 does not react with CO without a UV light source. Peroxide dianion is a key actor in many important systems, such as lithium-air batteries, where it is the primary discharge product.[33] CO, although not commonly observed or generated during typical lithium-air cell cycling, may be observed when a formamide solvent such as DMF[34] is used and its oxidation by peroxide dianion provides a possible route to lithium carbonate formation, a serious problem in current lithium-air cells.[35]

In conclusion, the encapsulation of peroxide dianion in the cavity of a hexacarboxamide cryptand results in an organic-solvent soluble source of peroxide dianion, permitting its intrinsic properties to be explored. The unprecedented oxidation of CO with a metal-free peroxide dianion results in the formation of carbonate which is also recognized by the anion receptor. Labeling studies confirm that the resulting carbonate is indeed derived from the coupling of peroxide and CO. Thus, transition metals are not an absolutely required ingredient in facilitating CO oxidation by peroxide dianion. Identification of this mode of reactivity may provide insight into decomposition modes operative in cycling lithium air cells, while serving to corroborate results from studies of peroxide dianion on CO-oxidizing ceria surfaces.

Acknowledgement This research was supported by the National Science Foundation (NSF) through the Centers for Chemical Innovation (CCI), Solar Fuels grant CHE-1305124 and U.S. DOE Office of Science under award DE-SC0009565 (DGN). Grants from the NSF also provided instrument support to the DCIF at MIT (Grants CHE-9808061 and DBI-9729592). The X-ray diffractometer was purchased with funding assistance from the NSF (Grant CHE-0946721). We are grateful to Michael Huynh for his assistance with NMR calculations, Rebecca de Las Cuevas for assistance with initial reactivity studies and Ioana Knopf for a gift of [PPN][HCO_3]. The authors also acknowledge the Robert Bosch Company for partial financial support.

Supporting Information Available: Provided are full details of experimental procedures for the synthesis of all new substances together with characterization data including details of X-ray diffraction studies and Cartesian coordinates for structures optimized by computational methods. This material is available free of charge via the Internet at `http://pubs.acs.org/`.

Notes and References

(1) (a) Benson, E. E.; Kubiak, C. P.; Sathrum, A. J.; Smieja, J. M. *Chem. Soc. Rev.* **2009**, *38*, 89–99; (b) Fujita, E. *Coord. Chem. Rev.* **1999**, *185-186*, 373 – 384; (c) Li, C. W.; Ciston, J.; Kanan, M. W. *Nature* **2014**, *508*, 504–507; (d) Torella, J. P.; Gagliardi, C. J.; Chen, J. S.; Bediako, D. K.; Coln, B.; Way, J. C.; Silver, P. A.; Nocera, D. G. *Proc. Natl. Acad. Sci. U.S.A.* **2015**, *112*, 2337–2342.

(2) Royer, S.; Duprez, D. *ChemCatChem* **2011**, *3*, 24–65.

(3) Haruta, M.; Kobayashi, T.; Sano, H.; Yamada, N. *Chem. Lett.* **1987**, *16*, 405–408.

(4) Kireev, A.; Mukhin, V.; Kireev, S.; Klushin, V.; Tkachenko, S. *Russ. J. Appl. Chem.* **2009**, *82*, 169–171.

(5) (a) Curtis, M. D.; Han, K. R. *Inorg. Chem.* **1985**, *24*, 378–382; (b) Ellul, C. E.; Saker, O.; Mahon, M. F.; Apperley, D. C.; Whittlesey, M. K. *Organometallics* **2008**, *27*, 100–108; (c) Blosser, P. W.; Gallucci, C., Judith; Wojcicki, A. *J. Mol. Cat. A: Chem.* **2004**, *224*, 133–144; (d) Ogasawara, M.; Maseras, F.; Gallego-Planas, N.; Kawamura, K.; Ito, K.; Toyota, K.; Streib, W. E.; Komiya, S.; Eisenstein, O.; Caulton, K. G. *Organometallics* **1997**, *16*, 1979–1993; (e) Letts, J. B.; Mazanec, T. J.; Meek, D. W. *Organometallics* **1983**, *2*, 695–704; (f) Siegl, W. O.; Lapporte, S. J.; Collman, J. P. *Inorg. Chem.* **1973**, *12*, 674–677; (g) Dzik, W. I.; Creusen, C.; de Gelder, R.; Peters, T. P. J.; Smits, J. M. M.; de Bruin, B. *Organometallics* **2010**, *29*, 1629–1641; (h) Siegl, W. O.; Lapporte, S. J.; Collman, J. P. *Inorg. Chem.* **1971**, *10*, 2158–2165; (i) Dzik, W. I.; Smits, J. M. M.; Reek, J. N. H.; de Bruin, B. *Organometallics* **2009**, *28*, 1631–1643; (j) Dürr, S.; Zarzycki, B.; Ertler, D.; Ivanović-Burmazović, I.; Radius, U. *Organometallics* **2012**, *31*, 1730–1742.

(6) (a) Lawson, H. J.; Atwood, J. D. *J. Am. Chem. Soc.* **1988**, *110*, 3680–3682; (b) Kelley, M. R.; Rohde, J.-U. *Inorg. Chem.* **2013**, *52*, 2564–2580; (c) Lawson, H. J.; Atwood, J. D. *J. Am. Chem. Soc.* **1989**, *111*, 6223–6227.

(7) Lu, Z.; Ma, D.; Yang, L.; Wang, X.; Xu, G.; Yang, Z. *Phys. Chem. Chem. Phys.* **2014**, *16*, 12488–12494.

(8) Choi, Y. M.; Abernathy, H.; Chen, H.-T.; Lin, M. C.; Liu, M. *ChemPhysChem* **2006**, *7*, 1957–1963.

(9) Pushkarev, V. V.; Kovalchuk, V. I.; d'Itri, J. L. *J. Phys. Chem. B* **2004**, *108*, 5341–5348.

(10) Zhao, Y.; Teng, B.-T.; Wen, X.-D.; Zhao, Y.; Chen, Q.-P.; Zhao, L.-H.; Luo, M.-F. *J. Phys. Chem. C* **2012**, *116*, 15986–15991.

(11) Lopez, N.; Graham, D. J.; McGuire, R.; Alliger, G. E.; Shao-Horn, Y.; Cummins, C. C.; Nocera, D. G. *Science* **2012**, *335*, 450–453.

(12) Ullman, A. M.; Sun, X.; Graham, D. J.; Lopez, N.; Nava, M.; De Las Cuevas, R.; Müller, P.; Rybak-Akimova, E. V.; Cummins, C. C.; Nocera, D. G. *Inorg. Chem.* **2014**, *53*, 5384–5391.

(13) Please see the SI for a line drawing of the hydrogen bonding anion receptor.

(14) Kang, S. O.; VanderVelde, D.; Powell, D.; Bowman-James, K. *J. Am. Chem. Soc.* **2004**, *126*, 12272–12273.

(15) TBA = Tetrabutylammonium, $N(Bu)_4{}^+$.

(16) Pramanik, A.; Emami Khansari, M.; Powell, D. R.; Fronczek, F. R.; Hossain, M. A. *Org. Lett.* **2014**, *16*, 366–369.

(17) Gilli, P.; Pretto, L.; Bertolasi, V.; Gilli, G. *Acc. Chem. Res.* **2009**, *42*, 33–44.

(18) Kang, S. O.; Hossain, M. A.; Bowman-James, K. *Coord. Chem. Rev.* **2006**, *250*, 3038–3052.

(19) Please see the SI for additional details.

(20) Wu, G. *Prog. Nucl. Magn. Reson. Spectrosc.* **2008**, *52*, 118–169.

(21) Smith, M.; Steuernagel, S.; Whitfield, H. *Solid State Nucl. Magn. Reson.* **1995**, *4*, 313–316.

(22) Leskes, M.; Drewett, N. E.; Hardwick, L. J.; Bruce, P. G.; Goward, G. R.; Grey, C. P. *Angew. Chem. Int. Ed.* **2012**, *51*, 8560–8563.

(23) Shima, T.; Hampel, F.; Gladysz, J. A. *Angew. Chem. Int. Ed.* **2004**, *43*, 5537–5540.

(24) Kong, X.; O'Dell, L. A.; Terskikh, V.; Ye, E.; Wang, R.; Wu, G. *J. Am. Chem. Soc.* **2012**, *134*, 14609–14617.

(25) PPN = Bis(triphenylphosphine)iminium, $[N(PPh_3)_2]^+$. [PPN][HCO_3] is prepared via a literature procedure[36].

(26) Brooks, S. J.; Gale, P. A.; Light, M. E. *Chem. Commun.* **2006**, 4344–4346.

(27) Akhuli, B.; Ravikumar, I.; Ghosh, P. *Chem. Sci.* **2012**, *3*, 1522–1530.

(28) Ravikumar, I.; Ghosh, P. *Chem. Commun.* **2010**, *46*, 1082–1084.

(29) Elbe, G. v. *J. Am. Chem. Soc.* **1932**, *54*, 821–822.

(30) Laming, F. P.; Buxton, G.; Wilmarth, W. K. *J. Phys. Chem.* **1969**, *73*, 867–873.

(31) Gorse, R.; Volman, D. *J. of Photochem.* **1972-1973**, *1*, 1–10.

(32) Kisacik, I.; Stefanova, A.; Ernst, S.; Baltruschat, H. *Phys. Chem. Chem. Phys.* **2013**, *15*, 4616–4624.

(33) Christensen, J.; Albertus, P.; Sanchez-Carrera, R. S.; Lohmann, T.; Kozinsky, B.; Liedtke, R.; Ahmed, J.; Kojic, A. *J. Electrochem. Soc.* **2011**, *159*, R1–R30.

(34) Chen, Y.; Freunberger, S. A.; Peng, Z.; Bardé, F.; Bruce, P. G. *J. Am. Chem. Soc.* **2012**, *134*, 7952–7957.

(35) Luntz, A. C.; McCloskey, B. D. *Chem. Rev.* **2014**, *114*, 11721–11750.

(36) Meckfessel, L. M. Synthesis and Reactivity of Tungsten(0) Hydroxo and Bicarbonato Complexes. Ph.D. thesis, Texas A&M, 1994.